Supporting Information

Palladium Modified Porous Silicon as Multi-functional MALDI chip for Serum Peptides Detection

Xiao Li †, Xiaoming Chen†, Jie Tan†, Xiao Liang*§ and Jianmin Wu*†

†Institute of Microanalytical System, Department of Chemistry, Zhejiang University, Hangzhou, 310058, China

§Department of General Surgery, Sir Run Run Shaw Hospital，School of Medicine, Zhejiang University,Hangzhou,310058

Email address: wjm-st1@zju.edu.cn

Supplementary Figures

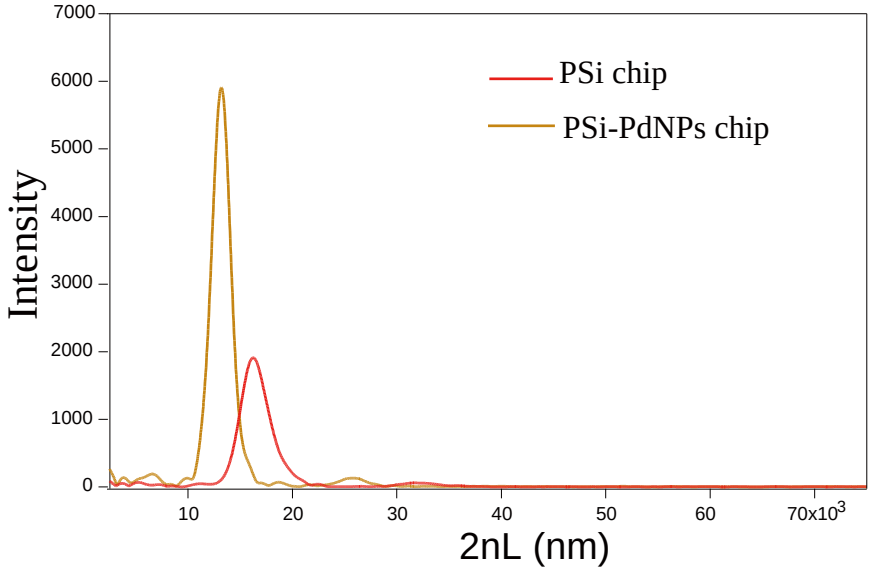

Fig. S1 Fourier transform reflectometric interference spectran FT-RIS) of PSi chip and PSi-PdNPs chip.The blue shift of FT-RIS peak indicated the refractive index of porous silicon layer significantly dcreased due to the coating of PdNPs on PSi surface[1].

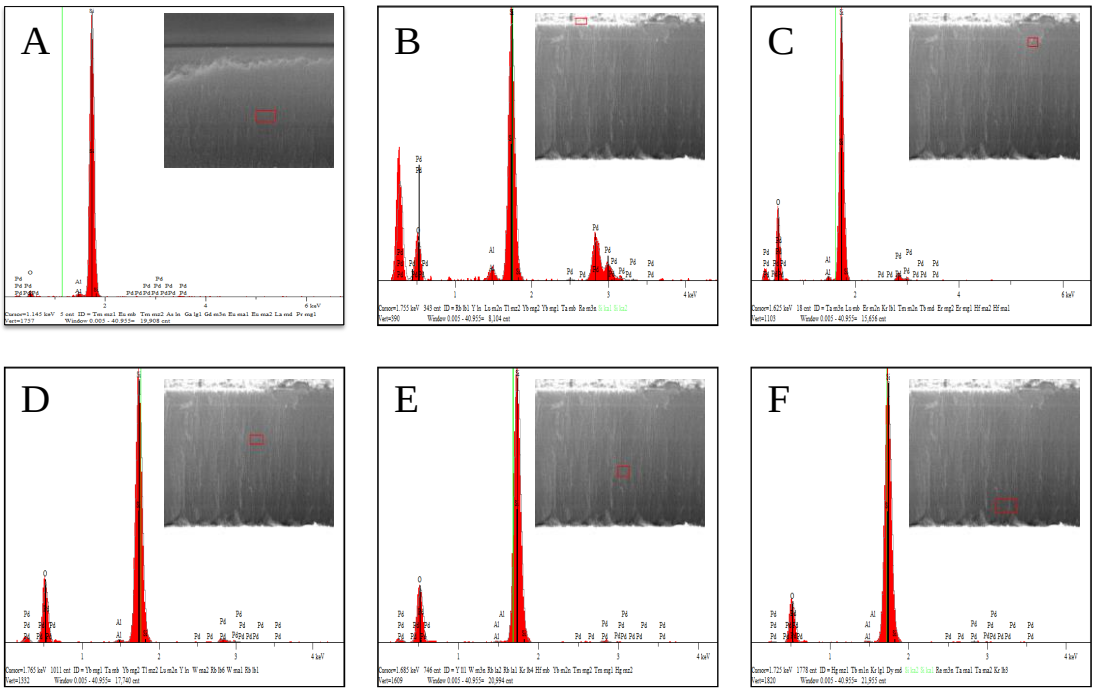

Fig. S2 Cross-sectional EDS profiling of PSi chip (A) and PSi-PdNPs chip (B,C, D, E, F) at different positions highlighted with rectanglar mark. The content of the palladilum element in PSi chip is 0.000% (A), while in the PSi-PdNPs chip the content is 40.068% (B), 9.007% (C), 5.480% (D), 2.951% (E) and 1.878% (F) from top surface to the bottom field.

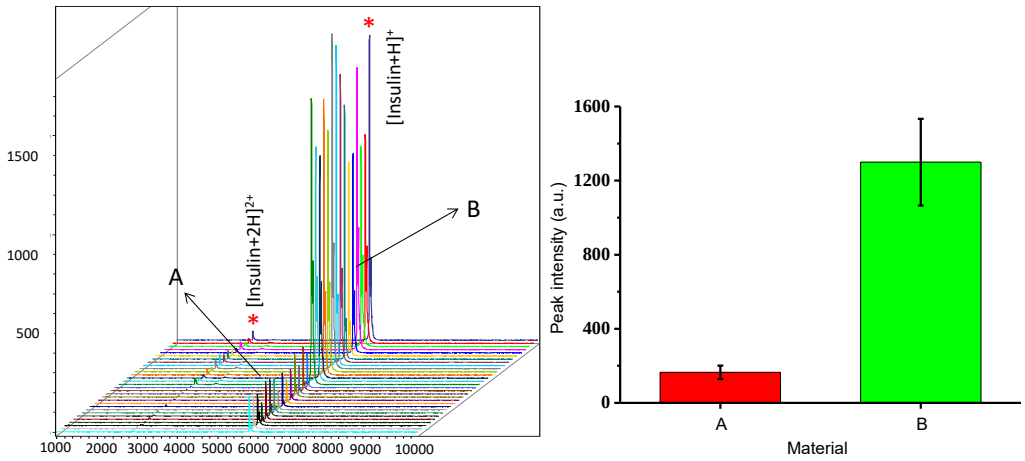

Fig. S3 Mass spectra and the peak intensity of the insulin samples obtained on the MALDI plate (A) and the PSi-PdNPs chip (B). 2 μL aliquot of the insulin sample (2.4 nmol/L in PBS) was spotted on the conventional MALDI-plate and PSi-PdNPs chip, respectively . The test was repeated for 15 times.

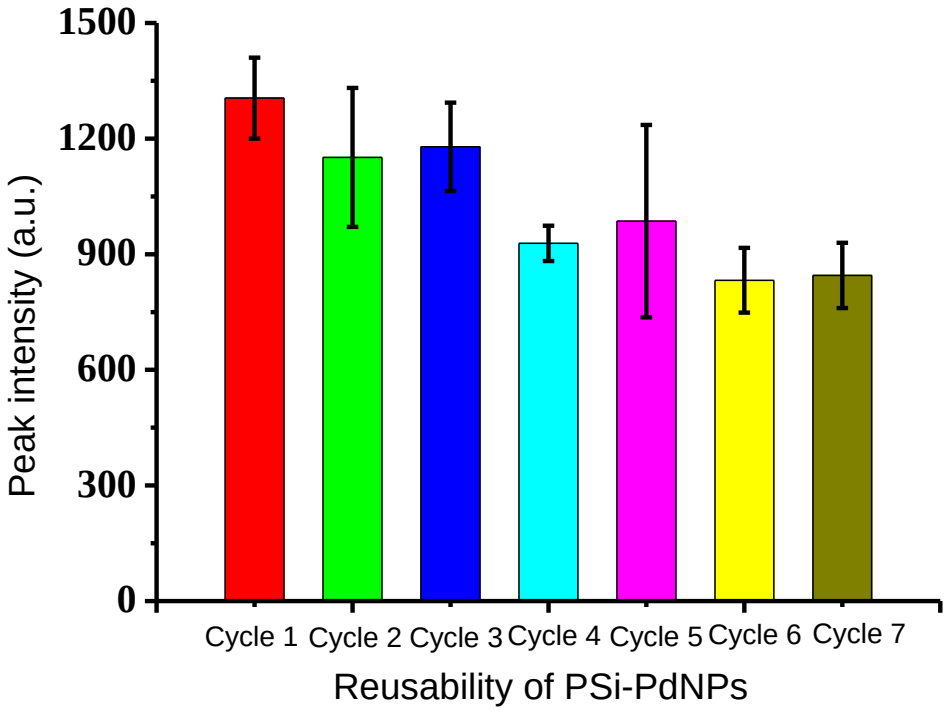

Fig. S4 Reusability of the PSi-PdNPs chip during the detection of insulin samples. In each cycle, 2 μL aliquot of the insulin sample (2.4 nmol/L in PBS) was spotted on the chip. After MS detection, the chip was treated with ultrasound in the eluent (H_2O: ACN: TFA = 50:50: 0.1, v/v/v) for 1 min and thereafter dried with N_2 gas. The test was repeated for 5 times in each cycle.

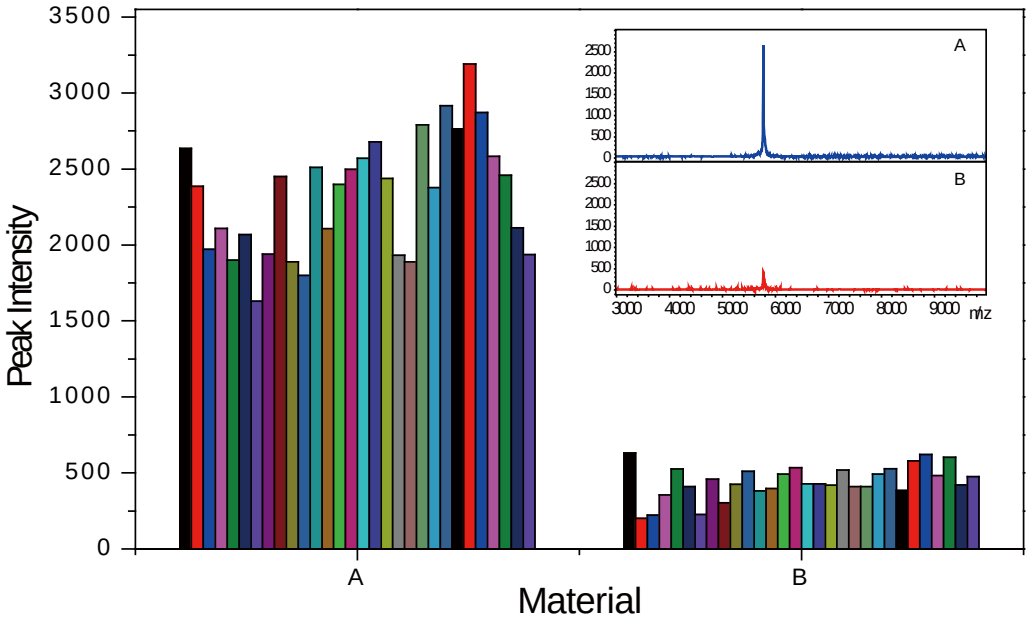

Fig. S5 Mass spectra of the insulin samples obtained on different PSi materials. 2 μL aliquot of the insulin sample was spotted on n-type PSi chip (A) and on n-type PSi-PdNPs chip (B), respectively. The test was repeated for 30 times on each chip.

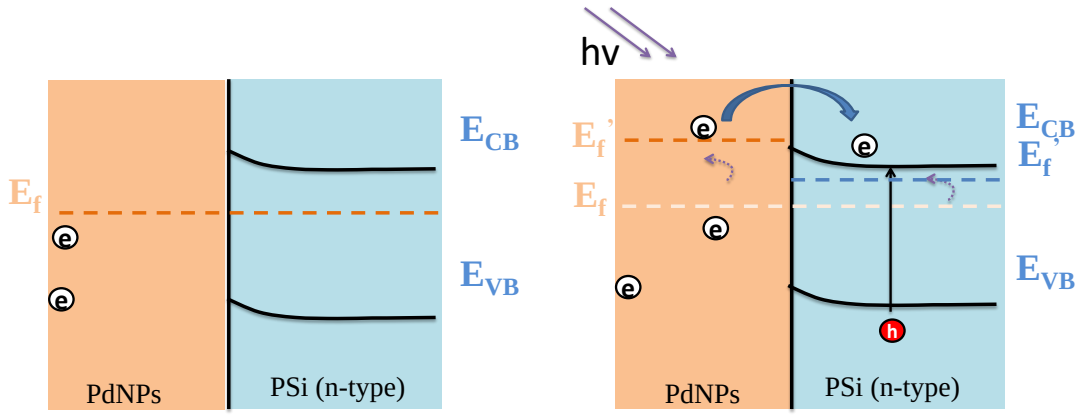

Charge equilibration before laser irradiation

Charge equilibration under laser irradiation

Fig. S6 Charge transfer diagram for PdNPs in contact with n-type PSi semiconductor under laser irradiation.

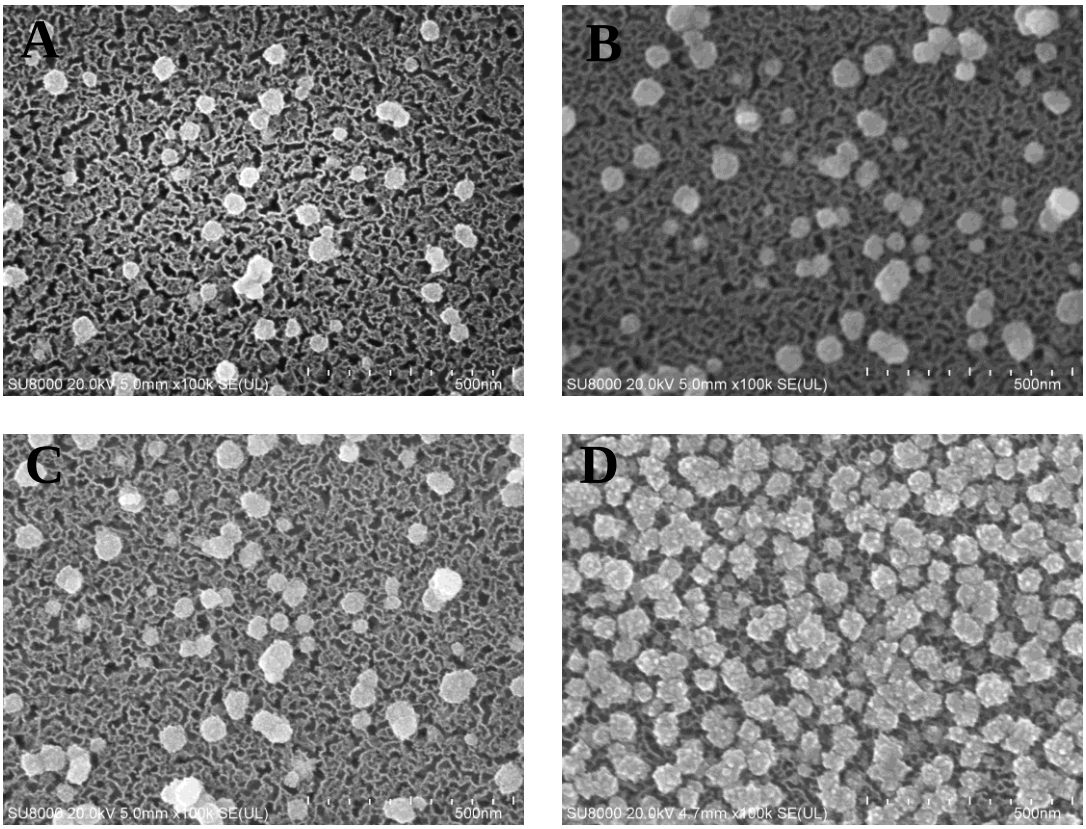

Fig. S7 The top view SEM image of PSi-PdNPs chip. The time for electrodeposition of PdNPs was controlled at (A) 1 min, (B) 10 min, (C) 15 min and (D) 20 min, respectively. The scale bar in the SEM image refers to 500 nm.

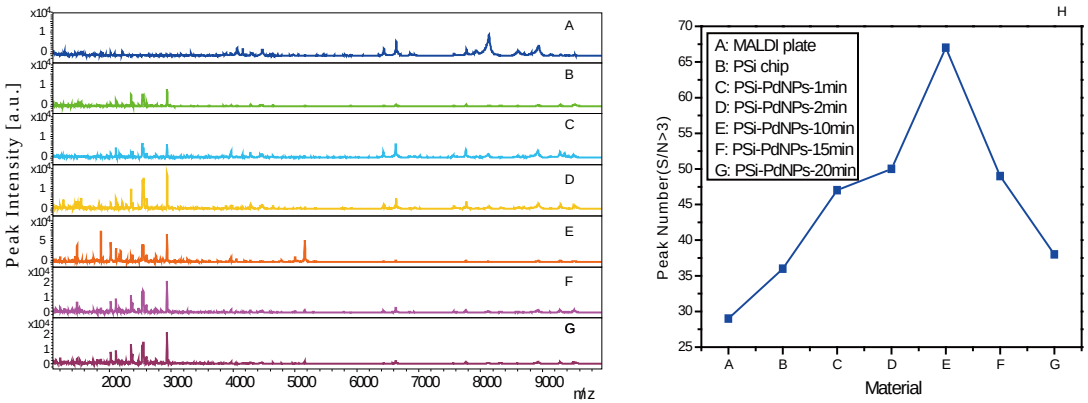

Fig. S8 Serum peptide spectra obtained on PSi-PdNPs chips with different Pd deposition time (A) standard MALDI plate, (B) PSi chip, (C) PSi-PdNPs chip (1 min), (D) PSi-PdNPs chip (2 min), (E) PSi-PdNPs chip (10 min), (F) PSi-PdNPs chips (15 min), (G) PSi-PdNPs chip (20 min), (H) The number of MS peaks with S/N > 3 obtained under different conditions corresponding to A-G.

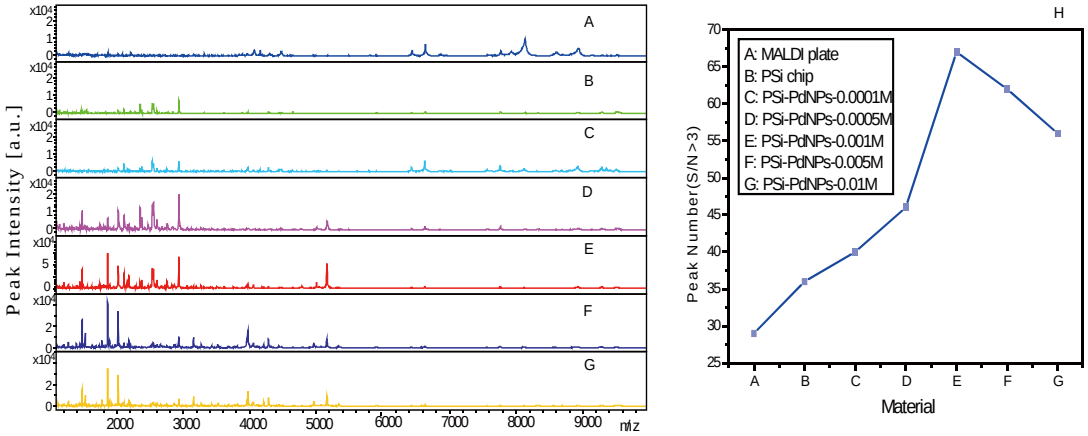

Fig. S9 Serum peptide spectra obtained on PSi-PdNPs chips prepared at different concentration of $PdCl_2$ solution. (A) standard MALDI plate, (B) PSi chip, (C) PSi-PdNPs chip (c = 0.0001 molL^{-1}), (D) PSi-PdNPs chip (c = 0.0005 mol L^{-1}), (E) PSi-PdNPs chip (c = 0.001 mol L^{-1}), (F) PSi-PdNPs chip (c = 0.005 mol L^{-1}), (G) PSi-PdNPs chip (c = 0.01 mol L^{-1}), (H) The number of MS peaks with S/N > 3 obtained under different conditions corresponding to A-G.

Table. S1 The number of detected peak（S/N > 3）obtained on different chip

MALDI	PSi chip	PSi-GNPs chip	PSi-PdNPs chip
—	1016.416	—	1016.972
—	—	1059.473	1059.104
—	1070.652	—	—
1076.428	1076.692	1076.578	1076.871
—	—	—	1275.226
—	—	1483.746	1483.325
—	—	—	1530.559
—	—	—	1545.021
		1739.368	
—	—	—	1778.781
1865.914	—	1865.624	1865.644
—	—	—	1887.848
—	—	—	1896.655
—	—	—	1933.949
—	—	—	1985.498
—	—	2005.291	2005.018
2023.583	2023.058	2023.678	2023.023
—	—	—	2044.146
—	—	—	2065.478
—	—	2083.344	2083.925
—	—	—	2168.586
		2113.914	
—	—	2184.754	2184.46
		2209.088	
—	2355.394	2355.298	2355.911
—	2539.553	—	2538.734
—	2556.365	—	2555.224
—	2934.9	2934.687	2934.968
—	—	3159.215	3159.23
3219.745	3219.507	—	—
—	—	—	3274.383
3318.856	3318.72	3318.347	3431.711
—	—	—	3524.496
—	—	—	3814.057
3886.417	3886.244	3886.365	—
—	—	3957.801	3957.498
3975.84	3975.524	3971.808	3975.26
—	—	—	4038.472
—	—	—	4055.09
4066.805	4066.81	4066.311	—
—	—	—	4113.819
—	—	4130.634	4130.634

4155.896	4155.14	4155.89	4155.997
—	—	—	4210.199
4283.92	4283.61	4283.019	4283.695
4302.685	4302.555	4302.655	4302.662
—	—	—	4326.461
—	4438.435	4438.231	4438.654
—	—	4468.639	4468.243
4647.548	4646.833	4646.153	4646.576
—	—	—	4788.262
—	—	—	4966.26
—	—	—	5005.478
—	—	—	5046.442
—	—	—	5069.818
—	—	—	5161.435
—	—	—	5202.996
—	—	5337.098	5337.914
—	5905.674	5905.128	5905.315
6434.751	6434.936	6434.551	6434.174
6635.051	6634.45	6634.058	6634.969
6855.356	—	—	—
—	6873.363	—	—
6935.702	6935.086	—	—
7023.054	7022.723	7022.781	7022.874
7567.681	7566.098	7565.29	7565.73
7771.783	7769.949	7769.268	7769.83
—	7938.236	7938.021	—
8130.24	8129.428	8129.228	8129.513
8605.477	8605.511	8605.142	8604.57
—	—	8690.722	8690.728
—	—	—	8888.575
—	—	8932.871	8932.278
8935.414	8935.363	8934.591	8934.911
9133.921	9132.631	9133.462	9133.561
9292.257	9291.207	9291.217	9291.06
9367.166	9365.203	—	9366.754
9421.732	—	—	9421.287
9496.896	9495.349	9495.12	9495.974
—	9515.321	—	9512.695

Reference

1. J. Feng, W.Zhao, B. Su, J. Wu, Biosensors and Bioelectronics 2011, 30: 21–27.